Journal of the Australian Ceramic Society (2019) 55:269–279
https://doi.org/10.1007/s41779-018-0232-1

RESEARCH

Biocompatibility of a PLA-based composite containing hydroxyapatite derived from waste bones of dolphin *Neophocaena asiaeorientalis*

Mi Rim Lee[1] · Gyung Won Lee[1] · Ji Eun Kim[1] · Woo Bin Yun[1] · Jun Young Choi[1] · Jin Ju Park[1] · Hye Ryeong Kim[1] · Bo Ram Song[1] · Ji Won Park[1] · Mi Ju Kang[1] · Yong Rock Ann[2] · Jung Youn Park[3] · Seung Yun Yang[1] · Dae Youn Hwang[1]

Received: 6 December 2017 / Revised: 13 June 2018 / Accepted: 21 June 2018 / Published online: 19 September 2018

Abstract

Natural hydroxyapatite (HA), derived from waste bones of several animal species, has received much attention as a material for bone grafts and fillers and has a role as a coating for metal implants because of its biocompatibility and non-toxicity. To investigate the applicability of HA derived from waste bones of novel animal sources, the biocompatibility and toxicity of a poly-L-lactic acid (PLA)-based composite containing HA derived from the backbone of the dolphin *Neophocaena asiaeorientalis* (HA_{NA}) were examined in Sprague-Dawley (SD) rats. HA_{NA} powder showed X-ray diffraction peak patterns that corresponded to those of standard HA. Among five composites prepared from different combinations of PLA and HA_{NA} (7:3, 6:4, 5:5, 4:6, and 3:7), a PLA/HA_{NA} composite manufactured with a 6:4 PLA:HA_{NA} ratio had high surface roughness (453 nm), 10.3 N of maximum load, and 451.9 MPa of module elasticity. After implantation in the subcutaneous region of SD rats for 8 weeks, the amount of confluent, aggregated structures of multilayered cells on the PLA/HA_{NA} implant surface was greater than that on the PLA surface, although both implants were completely covered with adhesive cells. During the implant period, the initial intact form of the PLA/HA_{NA} composite broke into small fragments with few inflammatory cells in the contact region and no indication of significant toxicity. Taken together, the results suggest that HA_{NA} may have good biocompatibility and be non-toxic as it did not induce an immune response in SD rats.

Keywords Hydroxyapatite · Dolphin *Neophocaena asiaeorientalis* · Waste bone · PLA composite · Biocompatibility

Introduction

Several body parts of whale including meat, oil, waxy substance, blubber, and baleen have been used for a variety of beneficial purposes for several centuries. Typically, whale meat and oil are used for human consumption, although they are uncommon foods in most of the world except Japan [1]. Spermaceti, a waxy substance from the head, and oil from sperm whales have been also used to make candles, soap, polishes, cosmetics, lamp fuel, and machinery lubricants [2]. Furthermore, whale blubber has been used as a source of components for soaps, oils, nutrient, and minerals, while baleen, a type of hair-like filter, had been used to make corsets, carriage springs, fishing poles, whips, and umbrella ribs until the start of the twentieth century [3]. However, whale bones have been of limited use, even though they account for 35–43% of the total body weight of whales [4]. After analyzing its composition, some studies have reported the possibility of using whale skeleton as a biofuel. Skeletal composition profiles, including lipid, protein, ash, and water in different skeleton elements, have been investigated in several species [5]. Whale bone is comprised of 42–48% of CaO, 26–28% of P_2O_5, 2.9–4.3% of SO_3, 1.2–3.7% of SiO_2, and 1.0–1.2% of Na_2O [6]. However, there are composition differences between dolphin and whale vertebrae. In particular, the lipid content of dolphin vertebrae is reported to be markedly lower than that of several species of whale, although other component content levels are similar in whale and dolphin species [5].

✉ Dae Youn Hwang
dyhwang@pusan.ac.kr

[1] Department of Biomaterials Science, College of Natural Resources & Life Science/Life and Industry Convergence Research Institute, Pusan National University, 50 Cheonghak-ri, Samnangjin-eup, Miryang-si, Gyeongsangnam-do 627-706, South Korea

[2] National Marine Biodiversity Institute of Korea, 75, Jangsan-ro 101beon-gil, Chungcheongnam-do 33662, Janghang-eup, Seocheon-gun, South Korea

[3] National Institute of Fisheries Science, 216, Gijanghaean-ro, Gijang-eup Gijang-gun, South Korea

Hydroxyapatite (HA) is a calcium phosphate-based inorganic material with structural and chemical similarity to the mineral phase of bone and teeth [7]. Currently, these are being widely used for bone grafts (dental, craniofacial, and orthopedic surgery), bone fillers, and as a coating for metal implants because they show good biocompatibility, bioaffinity, high osteoconductivity, non-toxicity, and have a non-inflammatory nature [8, 9]. Natural HA has been extracted from various waste bone sources including fish [4], bovine [10], tuna [11], and porcine [12] because the process for obtaining synthetic HA is either complex or unsafe [13]. Previous studies have focused on investigating the biocompatibility and bone formation characteristics of HA collected from waste bones of various animal sources [14]. However, little has been reported on the biocompatibility of HA composites or natural HA derived from the bone wastes of dolphin, even though HA density is greater in dolphin and whale bones than in fish and most mammalian bones [15].

In this study, we prepared a poly-L-lactic acid (PLA)-based composite containing HA derived from waste backbones of the dolphin *Neophocaena asiaeorientalis* (HA_{NA}). The PLA/HA_{NA} composite was investigated to determine its physicochemical properties, biodegradability, toxicity, and histocompatibility by performing subcutaneous implantation of PLA/HA_{NA} in Sprague-Dawley (SD) rats. The results revealed that HA purified from the backbone of dolphins has potential as a bio-based material for use in biomedical applications.

Materials and methods

Materials

The backbones of *N. asiaeorientalis* were kindly provided by the Whale Research Center of the National Institute of Fisheries Science, Korea. Bone samples were identified by Dr. Yong Rak Ann at the Whale Research Center in National Institute of Fisheries Science. Briefly, backbone samples were boiled at 100 °C for 2 h, then washed with a distilled water and acetone solution three times to remove proteins, lipids, and other debris. After drying at 160 °C for 48 h, the bones were ground in a pin mill machine (Daehwa, Yongin, Korea). To obtain HA_{NA}, the ground bones were washed with a 25 wt% NaOH solution (1:40 ratio) and neutralized with distilled water until pH 7 was achieved.

PLA was prepared by using ring-opening polymerization of L-lactide dimer as described previously [16]. Briefly, L-lactide dimer (3.46×10^{-2} mol), stannous octoate (1.40×10^{-4} mol), and acetic acid were completely mixed in toluene solvent, and the polymerization reaction was carried out under dry N_2 atmosphere at 110 °C for 48 h. After the reaction, PLA was harvested with deposition by using diethyl ether and subsequent filtration with Whatman filter paper (8 μm particle retention). The resultant product had a molecular weight (MW) of approximately 20,000.

Six different PLA/HA_{NA} mixtures were prepared by dissolving different ratios of PLA and HA_{NA} (7:3, 6:4, 5:5, 4:6, and 3:7) in a 10 wt% chloroform solution. The mixtures were then cast onto the glass plate of an automatic film coating apparatus (DAO-CO 02; Dao Technology, Hwaseong, Korea) to yield PLA/HA_{NA} composites with a thickness of approximately 0.1 mm. Following the removal of air bubbles in a vacuum oven, the glass plates bound with the PLA/HA_{NA} composite were immediately immersed in methanol and washed with distilled water until the solvent was completely removed. The PLA and the PLA/HA_{NA} composites used in the animal study were prepared as membranes with a 70% moisture content by dipping in a 1× phosphate-buffered saline (PBS) solution immediately before implantation under the skin of SD rats.

Mechanical characterization

The chemical composition of the HA_{NA} powder was analyzed by performing X-ray diffraction (XRD) with a Rigaku X-Ray Powder Diffractometer (Rigaku MSC, Woodlands, TX, USA). The peaks in the obtained XRD spectrum were compared with those on the JCPDS (1996) standard HA card [17].

Mechanical properties of the PLA/HA_{NA} composite, including tensile strength and maximum load, were measured as previously described [18, 19]. The strength and load levels were analyzed at 40 kV and 30 mA at room temperature under a velocity of 20 mm/min in a United SSTM-1 testing machine (United Calibration, Huntington Beach, CA, USA) with a 445 N load cell.

Contact angle analysis

Static contact angle measurements were obtained by using the sessile drop method and an OCA 15þ contact angle meter with a high-performance image-processing system (DataPhysics Instruments, Filderstadt, Germany). Firstly, a liquid (1 mL of glycerol or CH_2I_2, HPLC grade) was added to each sample by a motor-driven syringe at room temperature. The angles of the droplet on the surface were calculated by using ImageJ software (National Institutes of Health, Bethesda, MD, USA). The data presented are an average of five readings. Five samples of each material were measured, and three measurements were obtained from each sample.

Atomic force microscopy analysis

Prepared PLA and the PLA/HA_{NA} composite were frozen at − 70 °C for 24 h and then dehydrated for 3 days by using a

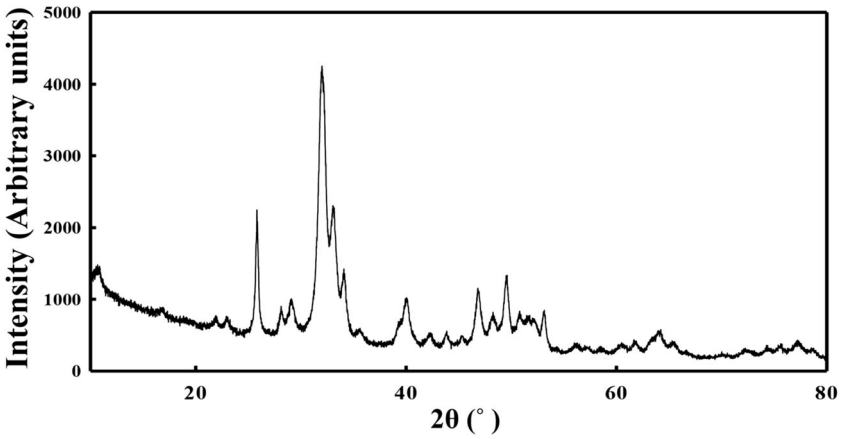

Fig. 1 X-ray diffraction spectrum of HA derived from the backbone of *N. asiaeorientalis*

lyophilizer (FDU-540, Tokyo Rikakikai, Tokyo, Japan). Dried samples were subsequently cut to 1 cm × 1 cm, after which a scan image was collected via atomic force microscopy (AFM) using an XE-100 microscope (Park Systems, USA) and standard AFM cantilevers with a specific scan speed (0.4 Hz), set point (16.16 nm), amplitude (22.34 nm), and a selected frequency (318.59E3 Hz) under atmospheric conditions at 25 °C. AFM images were analyzed by using Surface Xplore 1.3.11 (Micro Test Machines, Belarus). Surface morphology and surface profile were measured within a 30 μm × 30 μm area in triplicate. In addition, surface roughness values of PLA and the PLA/HA_{NA} composite were estimated from the AFM surface profile data by applying the root mean square formulation.

Microstructural characterization

To analyze the microstructural features of PLA and the PLA/HA_{NA} composite, samples were frozen at − 70 °C for 24 h, after which they were dehydrated in a lyophilizer for 3 days. The dried PLA and PLA/HA_{NA} were then coated with platinum (Pt) by using a sputter coater (Jeol JXA-840A; Jeol, London, UK) for 120 s under an argon atmosphere, after which they were observed via scanning electron microscopy (SEM) at 2000 × magnification (Stereoscan 250 MK III, London, UK) at 15 kV.

To observe alteration of the surface of PLA and PLA/HA_{NA} composite after implantation in SD rats for 8 weeks, each sample was removed from the incision pocket of the SD rat and dried. The dried PLA and PLA/HA_{NA} were then coated

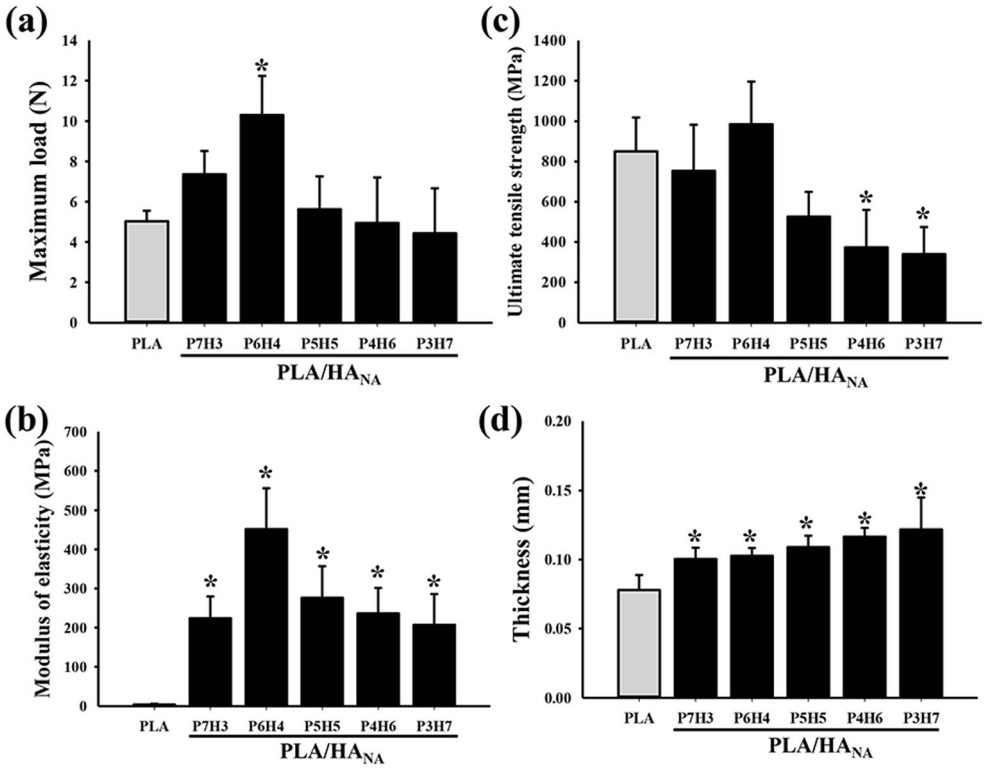

Fig. 2 Determination of an optimal combination of PLA and HA_{NA} for a PLA/HA_{NA} composite. **a** Maximum load, (*n*) ultimate tensile strength, **c** modulus of elasticity, and **d** thickness of PLA/HA_{NA} composites were measured using five different PLA and HA_{NA} combination ratios. Data presented as means ± SD of three replicates. *$p < 0.05$ compared to PLA

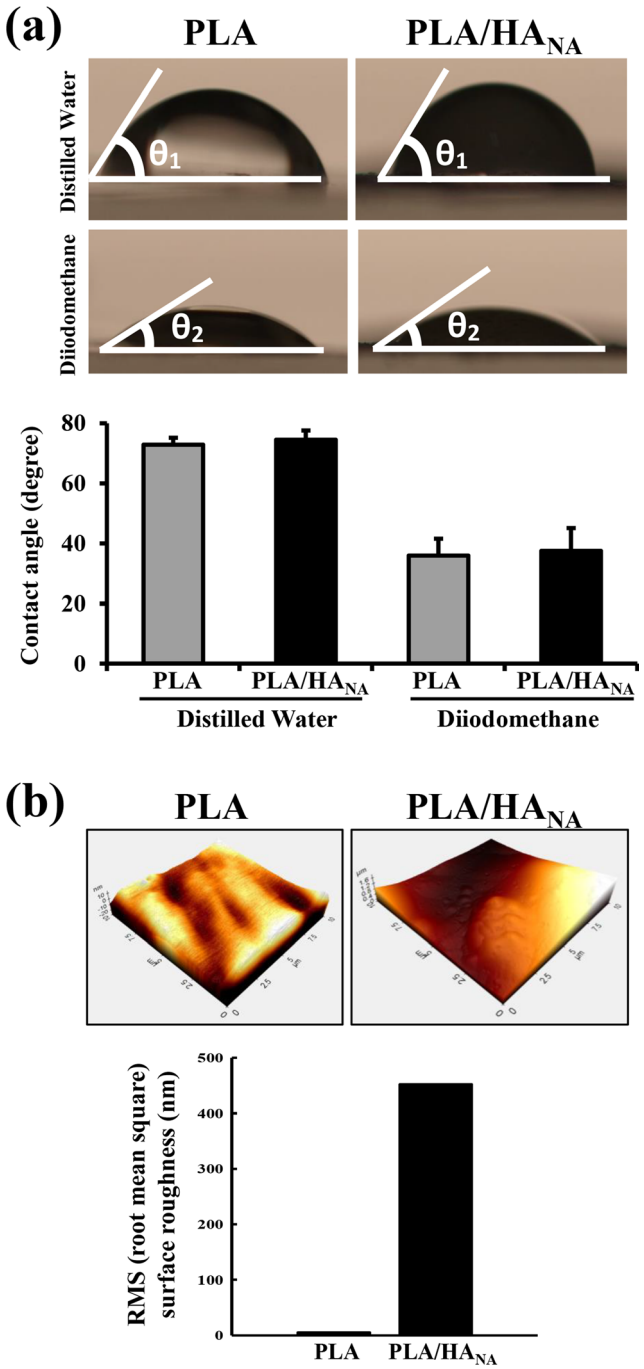

Fig. 3 Contact angle and AFM phase image of PLA/HA_{NA} composite. **a** Contact angles of PLA and PLA/HA_{NA} were measured in dH_2O and diiodomethane as described in "Materials and methods" section. Three to five samples were assayed in duplicate to determine contact angles. **b** 3D images of dried PLA and the PLA/HA_{NA} composite were analyzed by AFM using a 25 mm^2 scan size (3 mm × 3 mm). Surface roughness values for PLA and PLA/HA_{NA} were calculated from AFM data. Data presented as means ± SD of three replicates. *$p < 0.05$ compared to PLA

with Pt by using a sputter coater (Jeol JXA-840A) for 120 s under an argon atmosphere, after which they were observed by SEM at 2500 × or 5000 × magnifications (Stereoscan 250 MK III, London, UK) at 15 kV.

Animal study

The animal protocol used in our experiment was reviewed and approved by the Pusan National University-Institutional Animal Care and Use Committee (PNU-IACUC; approval PNU-2015-0972). Male SD rats (220–240 g body weight) were purchased from Samtako BioKorea Inc. (Osan, Korea) and handled at the Pusan National University Laboratory Animal Resources Center accredited by the Korea Food and Drug Administration (Accredited Unit 00231) and AAALAC International (Accredited Unit 001525). All animals were provided with ad libitum access to a standard irradiated chow diet (Samtako BioKorea Inc.) and water. During the experimental period, rats were maintained in a specific pathogen-free (SPF) state under a strict light cycle (lights on at 08:00 h and off at 20:00 h) at 23 ± 2 °C and 50 ± 10% relative humidity.

Eight-week-old SD rats were randomly divided into one of three groups ($n = 13–15$). The first group was subcutaneously implanted with PLA (PLA-implanted group), the second group was subcutaneously implanted with PLA/HA_{NA} (PLA/HA_{NA}-implanted group), and the third group was operated on in the same manner, but no composite was implanted (Sham-implanted group). The composites for implantation were prepared with a 0.1 mm thickness and were implanted after sterilization using 70% ethanol and 1× PBS. Prior to implantation, animals were anesthetized by intraperitoneal injection with Alflaxan (0.025 mL/100 g body weight). The skin was subsequently cleaned with 70% ethanol, after which a 2-cm-long incision was made on the midportion of the back. Next, composites were inserted into a subcutaneous pocket adjacent to the incision. Each rat received two implants, after which the incision was closed by using an Autoclip (Mikron, Precision, Canada). After 8 weeks, animals from each group were euthanized by using CO_2 gas. Each implant was collected from the incision pocket and underwent biodegradation and biocompatibility analysis. Additionally, whole blood, skin, liver, and kidney samples were immediately collected from euthanized SD rats implanted with PLA and PLA/HA_{NA} composite and stored at − 70 °C for analysis of serological components and histopathological factors.

Histological analysis

Skin with incision pocket as well as liver and kidney tissues were dissected from euthanized SD rats and fixed in 4% neutral-buffered formaldehyde (pH 6.8) overnight, after which each tissue was dehydrated and embedded in paraffin wax. Next, a series of tissue sections (4 μm thick) was cut from the paraffin-embedded tissue by using a Leica microtome (Leica Microsystems, Bannockburn, IL, USA). The sections were then deparaffinized with xylene, rehydrated with ethanol at gradual decreasing concentrations of 100–70%, and finally washed with distilled water. Slides bearing tissue

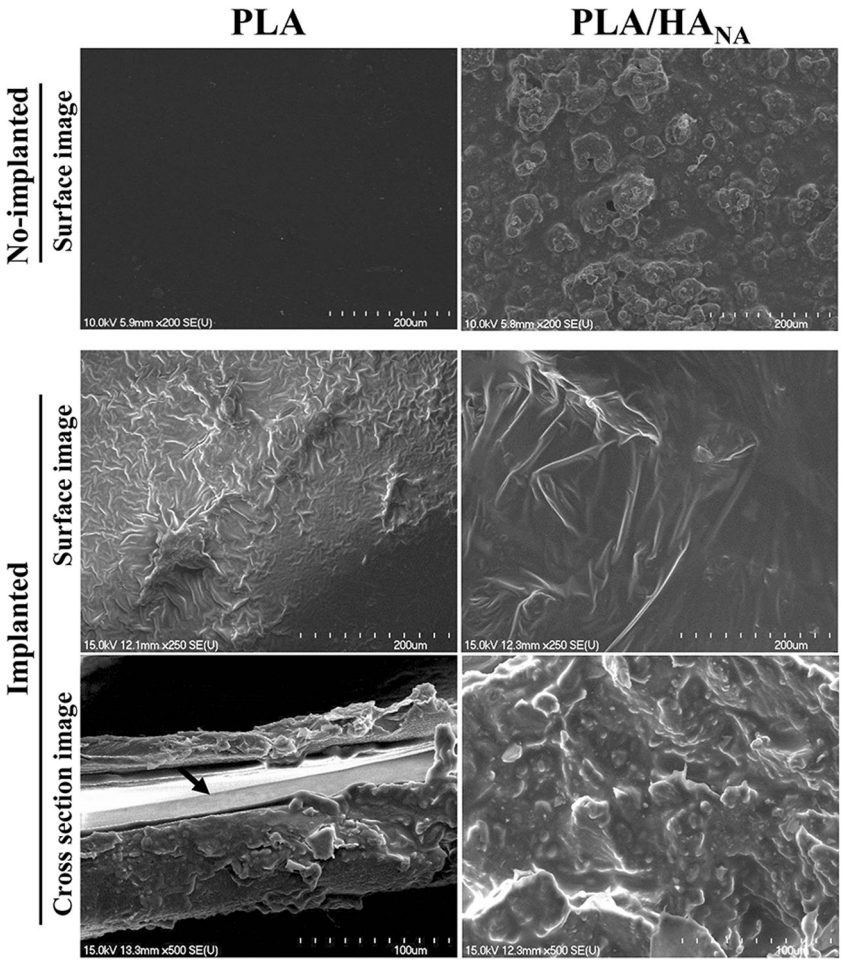

Fig. 4 SEM images of PLA and the PLA/HA$_{NA}$ composite before and after implantation in SD rats. Ultrastructures of PLA and PLA/HA$_{NA}$ surfaces were observed via SEM at 2000 ×, 2500 ×, or 5000 × magnifications as described in "Materials and methods". Three to five samples were assayed in duplicate for SEM analysis. Arrow indicates a PLA body

sections were stained with hematoxylin (Sigma-Aldrich Co., St. Louis, MO, USA) and eosin (Sigma-Aldrich Co.), then washed with dH_2O, after which histopathological changes were observed by using the Leica Application Suite (Leica Microsystems, Wetzlar, Germany).

Serum biochemical analysis

After fasting for 8 h prior to euthanatizing, whole blood from each rat in all groups was collected from their abdominal veins and incubated for 30 min at room temperature in a serum separating tube (BD Container, Franklin Lakes, NJ, USA). Serum was then obtained by centrifugation at 1500×*g* and analyzed for alkaline phosphatase (ALP), alanine aminotransferase (ALT), aspartate aminotransferase (AST), blood urea nitrogen (BUN), and creatinine (Crea) levels by using an automatic biochemical analyzer (BS-120, Mindray, China). All assays were conducted in duplicate and used fresh serum.

Statistical analysis

One-way analysis of variance (ANOVA) (SPSS for Windows, Release 10.10, Standard Version, Chicago, IL, USA) was used to identify significant differences between the sham and composite implantation groups or PLA- and PLA/HANA-implanted followed by Tukey post-hoc test for multiple comparison. All data were expressed as the means ± SD. A p value less than ($p > 0.05$) was considered statistically significant.

Results

Physicochemical properties of HA and PLA/HA$_{NA}$ composite

We investigated the chemical composition of the HA$_{NA}$ powder by using XRD. As shown in Fig. 1, all HA$_{NA}$ powder peaks corresponded to those of standard HA. In addition, to evaluate the optimal ratio of PLA to HA$_{NA}$ for the preparation of a PLA/HA$_{NA}$ composite, five different composites were prepared from PLA and HA$_{NA}$ powder, and their physicochemical properties including maximum load, tensile strength, modulus of elasticity, and thickness were measured. Among the tested combinations, the 6:4 PLA/HA$_{NA}$ ratio produced the highest maximum load level (10.4 N) and the greatest modulus of elasticity (451.9 MPa) (Fig. 2a, b). Tensile

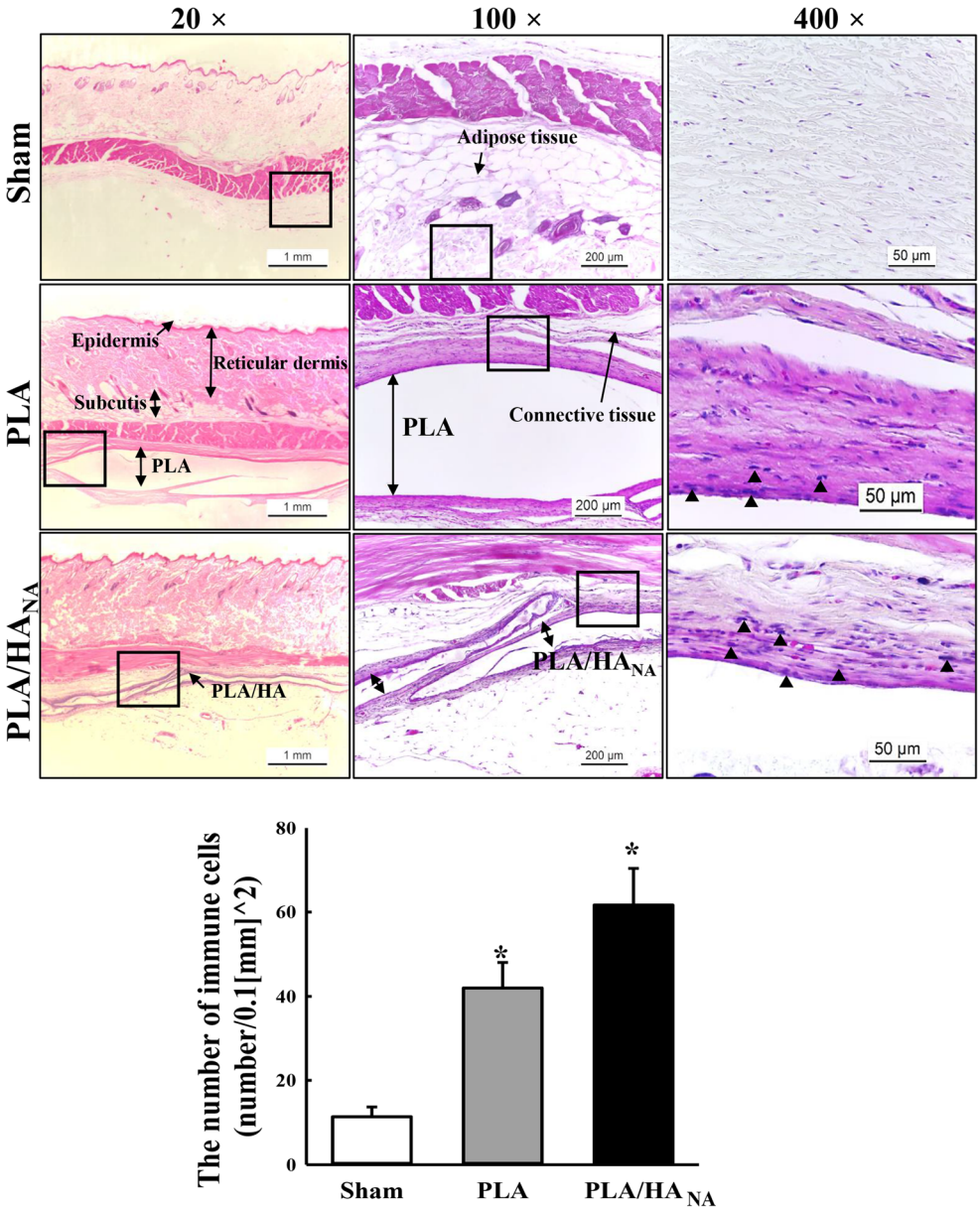

Fig. 5 Biocompatibility of PLA/HA_{NA} based on histological analysis. H&E-stained sections of subcutaneous tissue surrounding the PLA/HA_{NA} composite film implanted in SD rats for 8 weeks were observed via light microscopy at 20 ×, 100 ×, or 400 × magnifications. Rectangles in the images of the left and middle columns were magnified to form the images in middle and right columns, respectively. Arrowhead indicates immune cells

strength estimates were similar in the 7:3, 6:4, and 5:5 PLA/HA_{NA} composites but were significantly lower in the 4:6 and 3:7 PLA/HA_{NA} composites (Fig. 2c). All PLA/HA_{NA} composite thicknesses were consistent, although they were slightly thicker than that of PLA (Fig. 2d).

To investigate the cellular adhesiveness of the surface of the PLA/HA_{NA} composite, contact angle values and surface roughness were measured for both PLA and PLA/HA_{NA}. Any significant difference between PLA and PLA/HA_{NA} composite with the measured angles in the range of 69–79° and 25–48° was not detected in contact angle values with dH_2O (θ_1) and diiodomethane (θ_2) (Fig. 3a). However, a significant difference was detected in the AFM analysis of the surface roughness of the PLA and the PLA/HA_{NA} composite. The PLA/HA_{NA} appeared to be rougher, more irregular, and coarser than that of PLA; the PLA/HA_{NA} composite had a surface roughness of approximately 453 nm (Fig. 3b).

Taken together, these results suggest that pure natural HA_{NA} successfully extracted from the backbone of *N. asiaeorientalis* can be mixed with PLA at a 6:4 PLA:HA_{NA} ratio to form a PLA/HA_{NA} composite with good physical properties and effective cellular adhesiveness. Therefore, we used the 6:4 PLA:HA_{NA} composite to investigate its biocompatibility and toxicity in SD rats.

Biocompatibility of PLA/HA_{NA} composite under the skin of SD rats

To investigate the biocompatibility of the PLA/HA_{NA} composite after subcutaneous implantation into an animal, the

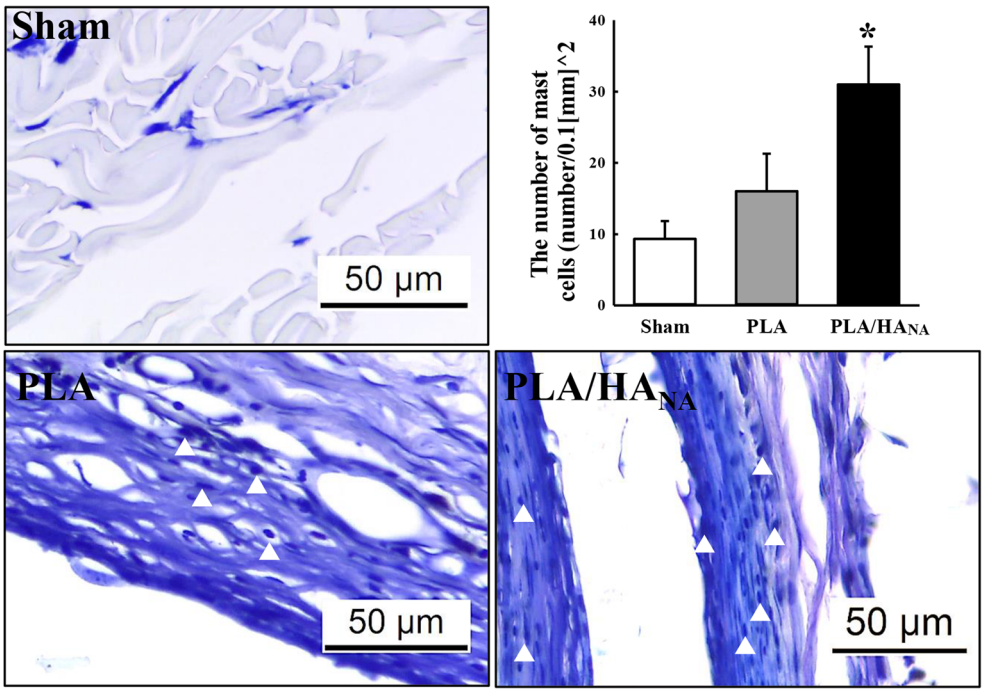

Fig. 6 Infiltration of mast cells into connective tissue surrounding the PLA/HA_{NA} implants. To determine the number of mast cells, slides with sections of skin tissue were stained with 0.25% toluidine blue and observed at 400 × magnification. The arrowhead indicates mast cells that have infiltrated the connective tissue within the dermis of the back skin of an SD rat. The total number of mast cells in a 0.1 mm^2 area of connective tissue was calculated by using the Leica Application Suite. Data presented as means ± SD from three replicates. *$p < 0.05$ compared to the Sham-implanted group. Arrowhead indicates mast cells

surface morphologies of PLA/HA_{NA} composite before and after implantation in SD rats were compared; as well, the histological structure of the SD rat skin adjacent to the implants was observed after implantation with PLA and the PLA/HA_{NA} composite for 8 weeks. The SEM image analysis of PLA/HA_{NA} composite before implantation showed jagged peaks and surface corrugations, while the PLA had a smooth surface (Fig. 4). After implantation, the surfaces of both PLA and the PLA/HA_{NA} composites were completely covered with adhesive cells indicating continuous cellular proliferation and spreading. The cells formed a confluent structure of multilayered cells with only a few aggregation structures observed. Both the degree of confluency and the amount of multilayered cell aggregations on the implant surface were greater on the PLA/HA_{NA} composite than on PLA (Fig. 4).

To investigate the inflammation around implantation site and degradation of PLA and the PLA/HA_{NA} composite, alterations in the histological structure of the skin adjacent to the implant pocket in the SD rats were examined. The surfaces of the PLA and PLA/HA_{NA} implants were well bonded to the connective tissue in the dermis of the skin, although the boundaries of both implants were clearly visible. However, there was a difference in the form of the two implants; the PLA implant maintained its complete initial form and was covered with adhesive cells, while the PLA/HA_{NA} composite was observed as several fragments (Fig. 5, left column). Immune cells in the skin tissue were abundantly and similarly distributed in the contact regions around both the PLA and PLA/HA_{NA} implants with no significant difference between the two (Fig. 5). However, there was a slightly higher number of mast cells in the PLA/HA_{NA}-implanted group than in the PLA-implanted group; specifically, there were more mast cells in the connective tissue around the PLA/HA_{NA} skin contact surface than in the PLA skin contact surface (Fig. 6). These data suggest that the PLA/HA composite has good biocompatibility in the subcutaneous tissue of SD rats and its presence does not induce severe infiltration of mast or immune cells.

Hepatotoxicity and nephrotoxicity of PLA/HA_{NA} composite

To investigate the hepatotoxicity and nephrotoxicity of the PLA/HA_{NA} composite, body weight, organ weight, histopathological tissue structure, and blood serum biochemical factors were examined in SD rats implanted with PLA and the PLA/HA_{NA} composite. No significant differences in body weight or weights of liver and kidney were observed among the Sham-, PLA-, or PLA/HA_{NA}-implanted groups (Table 1). In addition, the PLA- and PLA/HA_{NA}-implanted SD rats

Table 1 Alteration of body and organ weights of SD rats implanted with PLA/HA_{NA} for 8 weeks

Category	Sham	PLA	PLA/HA_{NA}
Body weight (g)	515.5 ± 89.80	543.18 ± 49.28	566.86 ± 51.57
Kidney (g)	0.66 ± 0.04	0.71 ± 0.05	0.66 ± 0.05
Liver (g)	4.00 ± 0.66	3.92 ± 0.71	3.72 ± 0.66

The data shown represent the means ± SD of three replicates

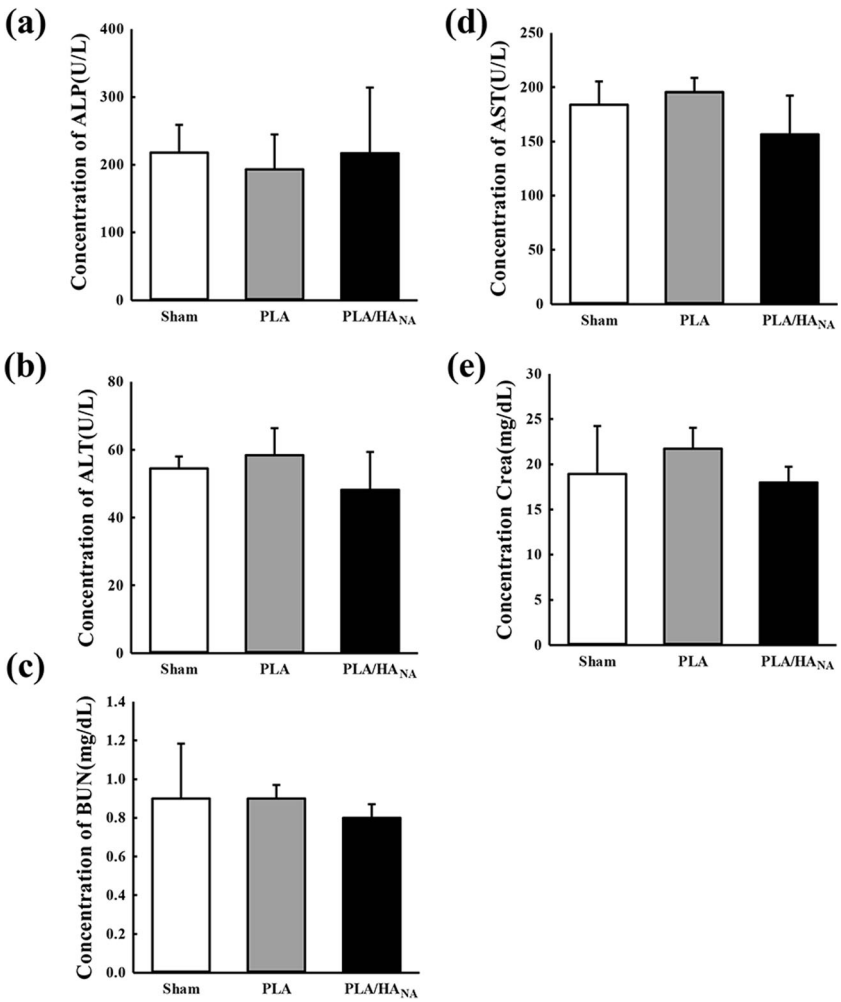

Fig. 7 Serum toxicity of the PLA/HA_{NA} composite in SD rats. Blood was collected from the abdominal veins of PLA- and PLA/HA_{NA}-implanted SD rats, and serum concentrations of **a** ALP, **b** AST, **c** ALT, **d** Crea, and **e** BUN were analyzed in duplicate by using a serum biochemical analyzer. Data presented as means ± SD of three replicates

exhibited no morphological differences in liver and kidney from those in the Sham-implanted group.

To evaluate whether PLA/HA_{NA} implantation for 8 weeks induced hepatotoxicity, alteration of the levels of several enzymes related to liver metabolism and changes in the histopathological structure of liver tissues were assessed in Sham-, PLA-, and PLA/HA_{NA}-implanted SD rats. No significant differences in liver toxicity indicators such as ALP, AST, and ALP were observed among the three groups (Fig. 7a–c). Furthermore, we investigated whether the lack of alteration of toxicity indicators in serum was reflected in the histopathological structure of liver tissue; there were no significant histopathological changes related to inflammation, necrosis, apoptosis, or fibrosis observed in the H&E-stained liver tissue of the PLA/HA_{NA}-implanted group (Fig. 8a).

Finally, nephrotoxicity of the implanted PLA/HA_{NA} composite was investigated in SD rats by assessing serum biochemical and histological features of the rat kidneys. BUN and Crea levels were similar in the Sham-, PLA-, and PLA/HA_{NA}-implanted groups with no significant differences detected (Fig. 7d, e). In addition, there were no specific pathological symptoms, including degeneration and necrosis of the glomerulus and renal tubes, observed in the kidney tissue of the PLA/HA_{NA}-implanted group (Fig. 8b).

Taken together, these results suggest that PLA/HA_{NA} implantation for 8 weeks does not induce hepatotoxicity or nephrotoxicity in SD rats.

Discussion

Recently, several surface treatment methods such as plasma, formation of a coating, and UV-ozone radiation have been used to treat biomaterial surfaces because, alone, most synthetic polymer surfaces can only support cell adhesion and proliferation within a limited range [20, 21]. In particular, PLA lacks a functional group required for cell interaction. An alkyl pendant group (CH_3) in the PLA backbone enhances the hydrophobicity of the polymer and induces the denaturalization of specific proteins for cell binding. However, addition of HA to PLA can improve the bioactivity of the composite through alteration of the surface's biochemistry from hydrophobic to hydrophilic [22]. During this process, the –OH group of HA mediates the binding of cell adhesion proteins

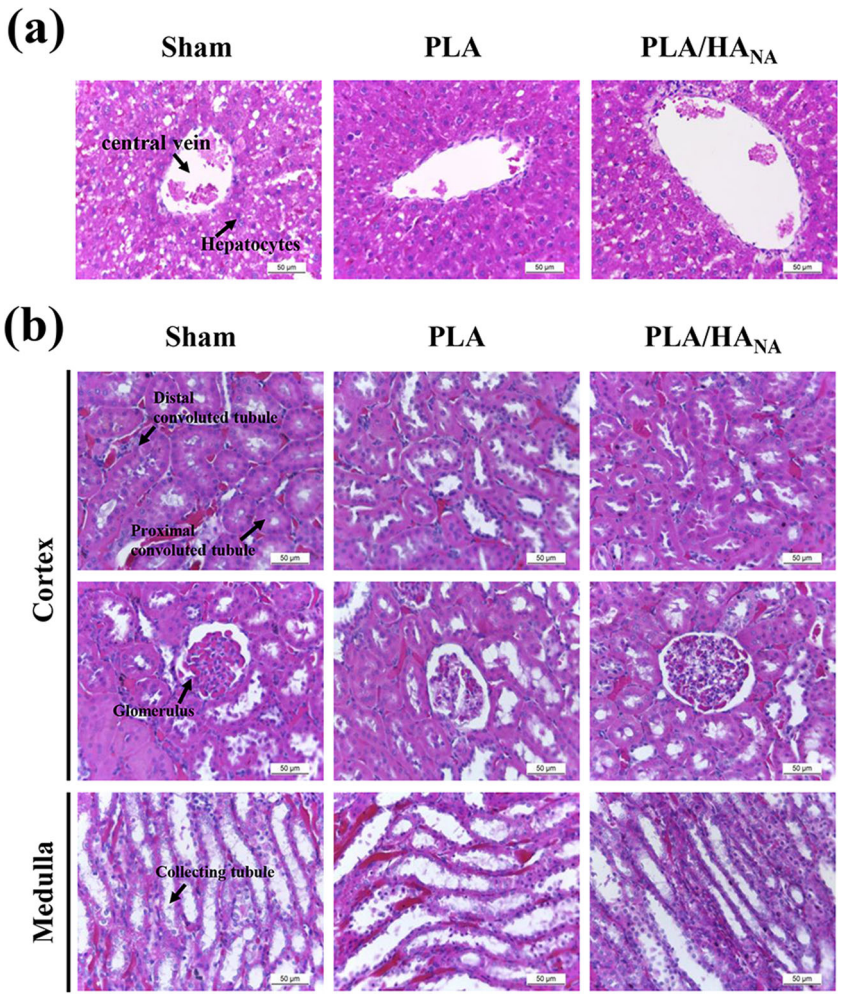

Fig. 8 Liver and kidney histological features following PLA/HA$_{NA}$ composite implantation in SD rats. Liver (**a**) and kidney (**b**) of SD rats were stained with H&E. Histological structures were viewed at 400 × magnification

including vitronectin and fibronectin and, subsequently, enhances the interaction between the cell membrane and PLA [23]. In this study, alterations in the physicochemical properties of a PLA-based composite were detected after addition of HA$_{NA}$ powder into the PLA. Among those properties, the maximum load, modulus of elasticity, and surface roughness were significantly increased in the PLA/HA$_{NA}$ (6:4) composite compared to those of the other tested composites. Such properties can contribute to enhancement of the biocompatibility of a PLA/HA$_{NA}$ composite. However, the addition of the –OH group in HA should be considered as one of the main factors enhancing cell adhesion between PLA/HA$_{NA}$ and the skin of SD rats, although more studies are needed to determine the level of cell interaction in implanted animals.

Until now, natural HA has been extracted from several bone types of several animal species by using specific processing methods. For example, pure natural HA has been extracted from bovine bones by using three different process; thermal decomposition, subcritical water, and alkaline hydrothermal processes. The chemical structure of the purified natural HA was very similar to that of the JCPDS standard HA card, regardless of the extraction method used [13]. As determined by XRD, the HA purified from pig bones at a high temperature maintained the chemical structure of standard HA [14]. Moreover, a porous structure with a sintered wall and a major crystalline phase were detected in HA derived from fish bone after heat treatment at 1300 °C [4]. Natural HA has been extracted from tuna bones and its properties were reported by Lee et al. [11]. In this study, we extracted natural HA$_{NA}$ from the waste backbones of *N. asiaeorientalis* by using an alkaline-based process. The chemical structure of the HA$_{NA}$ purified in this study was very similar to those reported in previous studies, although the animal sources and purity levels were different. The present study shows that dolphin bones can be an effective source of natural HA. However, there are limitations to the availability and sustainability of bones from dolphins; for example, *N. asiaeorientalis* was designated as endangered for a long time. Moreover, the ratio of bone weight to body weight is smaller in dolphins than in other mammals.

Different combinations of HA and various polymer materials have been applied as bone grafting materials during bone

regeneration and repair to overcome the disadvantages of HA [24]. Among the various polymer materials, PLA has been widely used as a binder for HA in order to enhance its resistance to shear forces and to support the survival and proliferation of skeletal stem cells [25]. Composites and scaffolds prepared with combinations PLA and HA show high degradation rates, good compatibility, and improved formation of mature bone in the absence of significant toxicity [26–29]. In particular, a composite consisting of 50% PLA and 50% nano-scale HA significantly enhanced the heterotrophic bone formation and ALP activity of human mesenchymal stem cells (hMSCs) after intramuscular implantation for 12 weeks [29]. Also, the activity of human osteoblasts (HOB) was higher on PLA combined with two different forms of HA than it was on PLA combined with tissue culture plastic [30]. In this study, the optimal combination of PLA and HA_{NA} was determined to be six parts PLA to four parts HA_{NA}. The 6:4 PLA/HA_{NA} composite showed the highest maximum load and the greatest modulus of elasticity when compared with other PLA/HA_{NA} ratios. However, the PLA-HA combination investigated in this study differs from those used in some previous studies [29]. We speculate that differences in the physical characteristics of PLA/HA combinations could be related to differences in the physicochemical properties of the HA being used. Regardless, the cell adhesion and structure confluency of the multilayered cells on the surface of the PLA/HA_{NA} composite observed in this study are in agreement with the enhanced activities of hMSCs and HOB cells observed for other PLA/HA composites [29, 30]. The results of this study indicate the possibility that HA_{NA} could be effectively combined with other polymers to manufacture an effective bone treatment composite.

The wettability and roughness of a composite surface are important factors when producing a biocompatible composite. Wettability is an important factor due to the direct relationship between water contact angle and cell adhesion. A high level of cell attachment can be obtained from contact angles between 40° and 80° [31]. Also, the surface roughness of a composite polymer can help to improve cell adhesion, growth, and proliferation [32, 33]. Similar results for the relationship between surface roughness and cell adhesion were detected in the present study. The roughness of the PLA/HA_{NA} composite was significantly greater than that of PLA alone, and the aggregation of multilayered cells was greater on the surface of the PLA/HA_{NA} composite than on the PLA surface. Therefore, the present study provides additional evidence that surface roughness of a PLA/HA composite is closely associated with cell adhesion.

Conclusion

In this study, we investigated the biocompatibility and toxicity of a PLA/HA_{NA} composite prepared by using HA derived from the waste bones of *N. asiaeorientalis* to determine if the derived composite could have potential medical application. The results provide the first scientific evidence that a PLA/HA_{NA} composite is biocompatible and does not induce toxicity or inflammation when subcutaneously implanted in SD rats for up to 8 weeks. Therefore, HA_{NA} can be considered a suitable material for use as a bone substitute. Such an application could be part of a strategy for the effective utilization of bone waste obtained from the seafood industry.

Acknowledgements We thank Jin Hyang Hwang, the animal technician, for directing the care and management of animals at the Laboratory Animal Resources Center in Pusan National University.

Funding This study was supported by grants to Professor Dae Youn Hwang from the Korea Institute of Planning & Evaluation for Technology in Food, Agriculture and Forestry (116027-032-HD030) and Basic Science Research Program through the National Research Foundation of Korea (NRF) funded by the Ministry of Education (2017R1D1A3B03032631).

References

1. Elvevoll, E.O., Sørensen, N.K., Osterud, B., Ofstad, R., Martinez, I.: Processing of marine foods. Meat Sci. (1996). https://doi.org/10.1016/0309-1740(96)00071-X
2. Gosho, M.E., Rice, D.W., Breiwick, J.M.: The sperm whale, *Physeter microcephalus*. Mar Fish Rev. **46**, 54–64 (1984)
3. Zelko, F.: From blubber and baleen to buddha of the deep: The rise of the metaphysical whale. Soc Anim. (2012). https://doi.org/10.1163/156853012X614387
4. Ozawa, M., Suzuki, S.: Microstructural development of natural hydroxyapatite originated from fish-bone waste through heat treatment. J Am Ceram Soc. (2002). https://doi.org/10.1111/j.1151-2916.2002.tb00268.x
5. Higgs, N.D., Little, C.T., Glover, A.G.: Bones as biofuel: a review of whale bone composition with implications for deep-sea biology and palaeoanthropology. Proc Biol Sci. (2011). https://doi.org/10.1098/rspb.2010.1267
6. Nemliher, J.G., Baturin, G.N., Kallaste, T.E., Murdmaa, I.O.: Transformation of hydroxyapatite of bone phosphate from the ocean bottom during fossilization. Lithol Miner Resour. (2004). https://doi.org/10.1023/B:LIMI.0000040736.62014.2d
7. Pandharipande, S., Sondawale, S.: Review on synthesis methods of hydroxyapatite and its biocomposites. Int J Sci Res Eng Technol. **17**, 3410–3416 (2016)
8. Elliott, J.C.: Structure and chemistry of the apatites and other calcium orthophosphates, Studies in Inorganic Chemistry, pp. 191–301. Elsevier, Amsterdam (1994)
9. Hulber, S.F., Bokros, J.C., Hench, L.L., Wilson, J., Heimke, G.: Ceramics in clinical applications: past, present and future. In: Vincenzini, P. (ed.) High Tech Ceramics, pp. 189–213. Elsevier, Amsterdam (1987)
10. Joschek, S., Nies, B., Krotz, R., Göpferich, A.: Chemical and physicochemical characterization of porous hydroxyapatite ceramics

made of natural bone. Biomaterials. (2000). https://doi.org/10.1016/S0142-9612(00)00036-3
11. Lee, C.K., Choi, J.S., Jeon, Y.J., Byun, H.G., Kim, S.K.: The properties of natural hydroxyapatite isolated from tuna bone. J Kor Fish Soc. 30, 652–659 (1997)
12. Xiaoying, L., Yongbin, F., Dachun, G., Wei, C.: Preparation and characterization of natural hydroxyapatite from animal hard tissues. Key Eng Mater. (2007). https://doi.org/10.4028/www.scientific.net/KEM.342-343.213
13. Barakata, N.A.M., Khila, M.S., Omrand, A.M., Sheikhd, F.A., Kim, H.Y.: Extraction of pure natural hydroxyapatite from the bovine bones bio waste by three different methods. J Mat Proc Technol. (2009). https://doi.org/10.1016/j.jmatprotec.2008.07.040
14. Haberko, K., Bucko, M.M., Brzezinska-Miecznik, J., Haberko, M., Mozgawa, W., Panz, T., Pyda, A., Zarebski, J.: Natural hydroxyapatite—its behaviour during heat treatment. J Eur Cer Soci. (2006). https://doi.org/10.1016/j.jeurceramsoc.2005.07.033
15. Hellmich, C., Ulm, F.J.: Average hydroxyapatite concentration is uniform in the extracollagenous ultrastructure of mineralized tissues: evidence at the 1-10μm scale. Biomechan Model Mechanobiol. (2003). https://doi.org/10.1007/s10237-002-0025-9
16. Kim, J.W., Kim, H.S.: Synthesis and characteristics of poly(l-lactic acid-block-γ-aminobutyric acid). Text Sci Eng. (2015). https://doi.org/10.12772/TSE.2015.52.053
17. JCPDS Card No. 9–432, 1996
18. Song, S.H., Kim, J.E., Lee, Y.J., Kwak, M.H., Sung, G.Y., Kwon, S.H., Son, H.J., Lee, H.S., Jung, Y.J., Hwang, D.Y.: Cellulose film regenerated from *Styela clava* tunics have biodegradability, toxicity and biocompatibility in the skin of SD rats. J Mater Sci Mater Med. (2014). https://doi.org/10.1007/s10856-014-5182-8
19. Seong, K.Y., Koh, E.K., Lee, S.H., Kwak, M.H., Son, H.J., Lee, H.S., Hwang, D.Y., Jung, Y.J.: Preparation and characterization of high absorptive cellulose film derived from *Styela Clava* tunic for wound dressing. Text Coloration Finish. (2015). https://doi.org/10.5764/TCF.2015.27.1.70
20. Palacio, M.L.B., Bhushan, B.: Bioadhesion: a review of concepts and applications. Phil Trans R Soc A. (2018). https://doi.org/10.1098/rsta.2011.0483
21. Alvarez-Barreto, J.F., Landy, B., VanGordon, S., Place, L., DeAngelis, P.L., Sikavitsas, V.I.: Enhanced osteoblastic differentiation of mesenchymal stem cells seeded in RGD-functionalized PLLA scaffolds and cultured in a flow perfusion bioreactor. J Tissue Eng Regen Med. (2011). https://doi.org/10.1002/term.338
22. Macha, I.J., Ben-Nissan, B., Santos, J., Cazalbou, S., Stamboulis, A., Grossin, D., Giordano, G.: Biocompatibility of a new biodegradable polymer-hydroxyapatite composite for biomedical applications. J Drug Deliv Sci Technol. (2017). https://doi.org/10.1016/j.jddst.2017.01.008
23. Thevenot, P., Hu, W., Tang, L.: Surface chemistry influences implant biocompatibility. Curr Top Med Chem. (2008). https://doi.org/10.1016/j.jddst/2017.01.008
24. García-Gareta, E., Coathup, M.J., Blunn, G.W.: Osteoinduction of bone grafting materials for bone repair and regeneration. Bone. (2015). https://doi.org/10.1016/j.bone.2015.07.007
25. Tayton, E., Purcell, M., Aarvold, A., Smith, J.O., Briscoe, A., Kanczler, J.M., Shakesheff, K.M., Howdle, S.M., Dunlop, D.G., Oreffo, R.O.: A comparison of polymer and polymer-hydroxyapatite composite tissue engineered scaffolds for use in bone regeneration. An *in vitro* and *in vivo* study. J Biomed Mater Res A. (2014). https://doi.org/10.1002/jbm.a.34926
26. Russias, J., Saiz, E., Nalla, R.K., Gryn, K., Ritchie, R.O., Tomsia, A.P.: Fabrication and mechanical properties of PLA/HA composites: a study of *in vitro* degradation. Mater Sci Eng C Biomim Supramol Syst. (2006). https://doi.org/10.1016/j.msec.2005.08.004
27. Barbieri, D., Renard, A.J., de Bruijn, J.D., Yuan, H.: Heterotopic bone formation by nano-apatite containing poly(D,L-lactide) composites. Eur Cell Mater. **19**, 252–261 (2010)
28. Zong, C., Qian, X., Tang, Z., Hu, Q., Chen, J., Gao, C., Tang, R., Tong, X., Wang, J.: Biocompatibility and bone-repairing effects: comparison between porous poly-lactic-co-glycolic acid and nano-hydroxyapatite/poly(lactic acid) scaffolds. J Biomed Nanotechnol. (2014). https://doi.org/10.1166/jbn.2014.1696
29. Canoux, C.B., Barbieri, D., Yuan, H., de Bruijn, J.D., van Blitterswijk, C.A., Habibovic, P.: *In vitro* and *in vivo* bioactivity assessment of a polylactic acid/hydroxyapatite composite for bone regeneration. Biomatter. (2014). https://doi.org/10.4161/biom.27664
30. Rizzi, S.C., Heath, D.J., Coombes, A.G., Bock, N., Textor, M., Downes, S.: Biodegradable polymer/hydroxyapatite composites: surface analysis and initial attachment of human osteoblasts. J Biomed Mater Res. (2001). https://doi.org/10.1002/1097-4636(20010615)55:4<475::AID-JBM1039>3.0.CO;2-Q
31. Wojcieszak, D., Mazur, M., Kalisz, M., Grobelny, M.: Influence of Cu, Au and Ag on structural and surface properties of bioactive coatings based on titanium. Master Sci Eng C. (2017). https://doi.org/10.1016/j.msec.2016.11.091
32. Khan, S.P., Auner, G.G., Newaz, G.M.: Influence of nanoscale surface roughness on neural cell attachment on silicon. Nanomedicine. (2005). https://doi.org/10.1016/j.nano.2005.03.007
33. Keshel, S.H., Azhdadi, S.N., Asefnejad, A., Sadraeian, M., Montazeri, M., Biazar, E.: The relationship between cellular adhesion and surface roughness for polyurethane modified by microwave plasma radiation. Int J Nanomedicine. (2011). https://doi.org/10.2147/IJN.S17180